

## Secondary Decays in Atmospheric Charm Contributions to the Flux of Muons and Muon Neutrinos

L. Pasquali<sup>1</sup>, M. H. Reno<sup>1,2</sup> and I. Sarcevic<sup>3</sup>

<sup>1</sup>*Department of Physics and Astronomy, University of Iowa, Iowa City, Iowa 52242*

<sup>2</sup>*CERN-TH, CH-1211 Geneva 23, Switzerland*

<sup>3</sup>*Department of Physics, University of Arizona, Tucson, Arizona 85721*

### Abstract

We present a calculation of the fluxes of muons and muon neutrinos from the decays of pions and kaons that are themselves the decay products of charmed particles produced in the atmosphere by cosmic ray-air collisions. Using the perturbative cross section for charm production, these lepton fluxes are two to three orders of magnitude smaller than the fluxes from the decays of pions and kaons directly produced in cosmic ray-air collisions. Intrinsic charm models do not significantly alter our conclusions, nor do models with a charm cross section enhanced in the region above an incident cosmic ray energy of 1 TeV.

### I. INTRODUCTION

The fluxes of atmospheric neutrinos and muons with energies larger than 100 GeV, which result from cosmic ray interactions with air molecules in the atmosphere [1,2], are measured in large underground detectors [3]. The fluxes are interesting for a variety of reasons, including the fact that the leptons are the decay products of particles produced in collisions with center of mass energies that may be extremely high. Cosmic rays, comprised primarily of protons, have been measured with energies up to  $E \sim 10^{20}$  eV [4], many orders of magnitude beyond the energies accessible in accelerator laboratories. In addition, atmospheric neutrinos and muons are a background for galactic and extra-galactic sources of neutrinos [5].

Atmospheric lepton fluxes come from two main sources. The so-called “conventional” atmospheric fluxes of muons and neutrinos come from hadronic production of  $K^\pm$ 's,  $K_L$  and  $\pi^\pm$ 's in cosmic ray-air collisions, followed by their leptonic, and in the case of kaons, semileptonic, decays. At the energies considered here,  $E > 10^2$  GeV, the magnitudes of the conventional lepton fluxes are governed by the lifetimes of the mesons. Because of time dilation, the decay lengths of these mesons are much larger than the depth of the atmosphere. A small fraction decay to leptons, but since they are copiously produced, the conventional flux dominates the lepton flux at the lower range of energies considered here. Given an

incident cosmic ray flux at the top of the atmosphere of  $\phi_{CR} \sim E^{-\alpha}$ , the flux of leptons from  $K$  and  $\pi$  decays has the energy dependence  $\phi_{\nu,\mu} \sim E^{-\alpha-1}$ . Values of  $\alpha$  are measured with  $\alpha \sim 2.7 - 3$  [6].

Charmed particle production and decay make important contributions to the lepton fluxes at high energies. Essentially all of the charmed particles decay in the atmosphere since  $\tau \sim 10^{-12}$  s, so these contributions are said to contribute to the “prompt” atmospheric flux. The energy behavior of the prompt fluxes is one power higher than the conventional fluxes for  $E < 10^7$  GeV:  $\phi_{\nu,\mu} \sim E^{-\alpha}$ . Even though charm production is suppressed relative to pion and kaon production, the energy behavior of the prompt flux means that the flux of leptons from charm decay dominates at high energies. In the recent work of Thunman, Ingelman and Gondolo [2], labeled here as TIG, a Monte Carlo model of atmospheric lepton production based on PYTHIA [7] was used to calculate the contribution of charmed particle semileptonic decays to the atmospheric flux.

Along with the semileptonic decays of charmed particles, in principle, secondary decays such as  $D \rightarrow K \rightarrow \mu\nu_\mu$  also contribute to the atmospheric lepton fluxes. Essentially all charmed meson decays have at least one kaon or pion in the final state, and the charged kaons and pions decay mainly to muons and neutrinos. It is the fluxes of these secondary muons and neutrinos from charm decay, and the more general topic of the uncertainties in the theoretical predictions for the atmospheric lepton fluxes from charm decay, that are the topics of this paper. We show that using the perturbative cross section for charm production, the secondary lepton fluxes are significant for  $E < 10^3$  GeV relative to the prompt fluxes, however they are small compared to the conventional fluxes. Even for strongly enhanced charm production, as long as the cross section is consistent with experimental measurements, the secondary lepton flux is negligible compared to the conventional flux.

In Section 2, we outline the standard calculational procedure, an approximate analytic method. Details of this procedure are outlined in Refs. [2,8,9]. We list our numerical inputs in Section 3 and present our results in Section 4. We follow with a summary in Section 5.

## II. CALCULATIONAL PROCEDURE

The calculations presented here are based on the cascade equations for baryon, meson and lepton fluxes [2,8,9]. The cascade equations describe the production of particle  $j$  through interactions and decays of particle  $k$ , and the loss of particle  $j$  through absorption and its own decay. The energy dependent flux of particles of type  $j$ ,  $\phi_j(E, X)$ , is governed in general by the equation

$$\frac{d\phi_j}{dX} = -\frac{\phi_j}{\lambda_j} - \frac{\phi_j}{\lambda_j^{(dec)}} + \sum_k S(k \rightarrow j) \quad (2.1)$$

where  $X$  is the column depth (slant depth) in the atmosphere measured from the top of the atmosphere,  $\lambda_j$  is the hadronic interaction length and  $\lambda_j^{(dec)} \sim \gamma c\tau_j$  is the decay length, all converted to units of g/cm<sup>2</sup>. The column depth is dependent on the incident angle. For vertical fluxes evaluated at sea level, the column depth is  $X = X_0 = 1300$  g/cm<sup>2</sup>. The quantity  $S(k \rightarrow j)$  describes the source of particles of type  $j$  from interactions or decays of particles of type  $k$ . For neutrinos and muons at energies above 100 GeV, since the interaction

and decay lengths are essentially infinite, only the source terms appear on the right hand side of equation (2.1). The source terms have the form:

$$S(k \rightarrow j) = \langle N_j \rangle \int_E^\infty dE_k \frac{\phi_k(E_k, X)}{\lambda_k(E_k)} \frac{dn_{k \rightarrow j}(E; E_k)}{dE}, \quad (2.2)$$

where  $\lambda_k(E_k)$  is an interaction length or decay length, depending on the source. The quantity  $dn_{k \rightarrow j}/dE$  describes the energy distribution of the produced particle  $j$ , and  $\langle N_j \rangle$  is the particle multiplicity. For decays, the value of  $\langle N_j \rangle$  is unity, except for pions. For the production of charm,  $\langle N_c \rangle = 2$ .

In principle, the cascade equations are a coupled set of equations. We make several simplifying assumptions so that we can solve the equations analytically. First, we decouple the meson equations, with the exception of charm decay to pions and kaons. In principle, there are interaction terms such as  $S(\pi \rightarrow K)$ , however, these are small compared to  $S(p \rightarrow K)$ , so we neglect the former. With this assumption, we can solve for conventional  $\pi$  and  $K$  fluxes separately, then evaluate their contributions separately to the neutrino and muon fluxes. The same holds true for charm production. We follow the produced charm in their decays to leptons, pions and kaons.

To further simplify the calculation, we represent the cosmic ray flux by the proton flux. The cosmic ray composition is dominantly protons [10], so the treatment of cosmic rays as protons is reasonable. This approximation was used by TIG in Ref. [2]. A feature that allows us to approximately solve the cascade equations is to use a factorization of the energy dependence in the fluxes. By writing

$$\phi_j(E, X) \equiv f_j(E, X)E^{-\beta_j}, \quad (2.3)$$

and assuming that  $f_j(E, X)$  is weakly dependent on energy, approximate solutions to the cascade equations are straightforward and lead to the power law energy behavior described in the introduction. Thunman, Ingelman and Gondolo have demonstrated this is a good approximation by comparing the approximate solutions to Monte Carlo results [2]. This is especially useful because the source terms factorize to

$$S(k \rightarrow j) = \frac{f_k(X)E^{-\beta_k}}{\lambda_k(E)} Z_{kj}(\beta_k, E) \quad (2.4)$$

where  $Z_{kj}(\beta_k, E)$  depends only weakly on energy. The calculation of the  $Z$ -moments is the essential ingredient in addition to  $\lambda$  to describe the lepton fluxes. The interaction moments include information about multiplicity, the magnitude and energy dependence of the relevant cross section and the energy distribution of the emerging particle. To simplify notation, we omit the energy argument in  $Z$ 's, although we do include energy dependent  $Z$ 's in our evaluation of the fluxes.

With the assumptions above, the solutions for the hadron fluxes are straightforward. For cosmic ray protons,  $\lambda_p^{(dec)}$  is infinite, and the solution for the flux is

$$\phi_p(X, E) = f_p(X)E^{-\alpha} = f_p(0)e^{-X/\Lambda_p}E^{-\alpha} \quad (2.5)$$

for  $\Lambda_k \equiv \lambda_k/(1 - Z_{kk})$ . For hadrons other than the proton, the solutions to the factorized cascade equations have two different forms, depending on whether one is in the high or

low energy regime. The energy regime is determined by whether or not the decay length of the particle is large compared to the column depth. The cascade equations are solved approximately in these two regimes, then interpolation between high and low is done with

$$\phi_j = \frac{\phi_j^{low} \phi_j^{high}}{\phi_j^{low} + \phi_j^{high}}. \quad (2.6)$$

Explicit solutions appear, for example, in Ref. [8]. The fluxes from each source are evaluated this way, then summed to get the total flux.

The lepton fluxes come from hadron decays, where the hadron fluxes are approximated via Eq. (2.6). In the high and low energy regimes, the approximate lepton fluxes can be written in simple form. For definiteness, we write the flux for neutrinos. The flux for muons is in exactly the same form. At high energies, the (direct) flux from source terms  $p \rightarrow j \rightarrow \text{leptons}$  is

$$\phi_\nu^{j,high}(X, E) = f_\nu^{j,high}(E, X) E^{-\alpha-1} = \frac{Z_{pj}(\alpha) Z_{j\nu}(\beta_j) \ln(\Lambda_j/\Lambda_p)}{1 - Z_{pp}(\alpha)} \frac{f_p(0)}{\lambda_j^{(dec)} \rho(X)} E^{-\alpha}, \quad (2.7)$$

where  $\rho(X)$  is the density of air at column depth  $X$ . The energy dependence of  $\lambda_j^{(dec)}$  makes the flux of leptons from high energy hadron decays suppressed by one power of energy relative to the proton flux. For low energies, the hadron flux itself is proportional to  $\lambda_j^{(dec)}$  and the decay length cancels. The energy dependence of the lepton flux tracks that of the primary cosmic ray proton flux. From the direct decays of low energy hadrons  $j$ ,

$$\phi_\nu^{j,low}(X, E) = f_\nu^{j,low}(E, X) E^{-\alpha} = \frac{Z_{pj}(\alpha) Z_{j\nu}(\beta_j)}{1 - Z_{pp}(\alpha)} f_p(0) E^{-\alpha}, \quad (2.8)$$

As indicated earlier, pions and kaons have relatively long lifetimes, so for  $E > 10^2$  GeV, they are “high energy” hadrons resulting in a lepton flux proportional to  $E^{-\alpha-1}$ . Charmed hadrons, for most of the energy range  $E \sim 10^2 - 10^8$  GeV, are low energy particles, so the resulting lepton flux has the low energy form proportional to  $E^{-\alpha}$ .

The extensions of these equations for secondary leptons from  $p \rightarrow \text{charm} \rightarrow j \rightarrow \text{leptons}$  is straightforward. The substitution

$$Z_{pj}(\alpha) \rightarrow Z_{pk_c}(\alpha) Z_{k_c j}(\beta_{k_c}) \quad (2.9)$$

is required for hadrons  $j$  that come from charmed particle ( $k_c$ ) decays. The calculation of the moments for direct processes have be done with a variety of assumptions [8,2]. It remains to indicate the inputs for interaction lengths and  $Z$ -moments and to describe our calculation of  $Z_{k_c j}(\beta_{k_c})$ .

### III. INPUTS

Eqs. (2.7) and (2.8) govern the lepton fluxes, with the additional substitution of Eq. (2.9) for the secondary fluxes. We use TIG parameters where they are available [2]. TIG have shown that for conventional charm production,  $D^\pm$ ,  $D^0$  and  $\bar{D}^0$  decays dominate the

sources of prompt leptons for most of the energies between  $10^2 - 10^8$  GeV. Consequently, we consider charm contributions only via  $D^\pm$ ,  $D^0$  and  $\bar{D}^0$  decays. Henceforth, we will only refer to particles, however, all of our calculations include both particles and antiparticles. The inputs fall into three categories: the incident proton flux (we assume that cosmic rays are protons), interaction  $Z$ -moments and interaction lengths, and decay  $Z$ -moments and decay lengths.

The incident flux of protons at the top of the atmosphere, following TIG, is taken to be isotropic, with

$$\phi_p(E, X = 0)[\text{cm}^{-2}\text{s}^{-1}\text{sr}^{-1}\text{GeV}^{-1}] = \begin{aligned} & 1.7 (E/\text{GeV})^{-2.7} & E < E_0 \\ & 174 (E/\text{GeV})^{-3} & E \geq E_0, \end{aligned} \quad (3.1)$$

with  $E_0 = 5 \cdot 10^6$  GeV.

The interaction lengths for the protons, pions and kaons require the total scattering cross sections with isoscalar nucleons. We use the Donnachie-Landshoff parameterization [11]

$$\sigma_{tot} = X s^\epsilon + Y s^{-\eta} \quad (3.2)$$

and the values of the parameters from the Particle Data Book [12] for incident protons,  $\pi^+$  and  $K^+$ . We use the  $K^+$  cross sections for  $K_L$ ,  $D^0$  and  $D^+$  as well. The cross sections are then rescaled with a constant factor of  $A^{2/3}$ , where  $A = 14.5$  is the average atomic number of air nuclear targets. Interaction  $Z$ -moments have been presented as a function of energy in Ref. [2] for nucleons, pions, kaons and  $D$  mesons. We use these  $Z$ -moments to evaluate Eqs. (2.7) and (2.8).

For particle lifetimes and branching fractions, we use the Particle Data Book values. The two-body decay moments for pion and kaon decays are straightforward to calculate. Formulae appear in Ref. [8], and numerical values, depending on the energy behavior of the decaying mesons, appear in Refs. [8] and [2]. For semileptonic and non-leptonic decays, the calculations are less obvious. These must be done for the decay moments for charm to pions and kaons, muons and neutrinos. An accurate evaluation of  $Z_{kej}(\beta_c)$  is difficult because the hadronic decay distributions cannot be calculated analytically. Data exist on distributions in charmed particle decays, for example, the  $K^\pm$  and  $K^0$  momentum spectra for  $D^0$ ,  $D^+$  and  $D_s^+$ , where the  $D$ 's are all produced approximately at rest [13]. The data are not immediately translatable into decay  $Z$ -moments because one must boost to the frame where the kinetic energies of the  $D$ 's are large.

For the simplest case of semileptonic charm decays, TIG distribute lepton momenta according to a weak matrix element

$$|\mathcal{M}|^2 = (p_D \cdot p_\mu)(p_\nu \cdot p_h) \quad (3.3)$$

where  $h$  is the final state hadron system. They find that the decay moments to muons and neutrinos are equal to within 15% for  $D$  mesons, and that the moments decrease by a factor of  $\sim 3$  as the  $D$ 's make the transition from the low energy to high energy regime.

The matrix element in Eq. (3.3) does not account for form factor modifications of the hadron weak vertex. To look at the sensitivity of the decay moment to the energy distribution, we have calculated the decay  $Z_{D^\pm\nu}$  using three-body phase space to dictate the energy distribution of the neutrino. Our results are shown in Fig. 1 by the points. The

energy dependence comes from the changing energy behavior of the  $D^\pm$  flux. The upper dashed line is the TIG result with  $\beta_D = 1.7$ , appropriate for low energy  $D$ 's, for example, at  $E = 10^2$  GeV. The lower dashed line is with  $\beta_D = 3$ , appropriate for high energy  $D$ 's, namely at  $10^8$  GeV. Over the range of energies between  $10^2 - 10^8$  GeV, there is a factor of  $\sim 2 - 2.4$  between the phase space result and the relevant TIG numbers. This factor of  $2 - 2.4$  gives a qualitative estimate of the uncertainty in the decay moments. We use the TIG semileptonic decay moments, interpolating between  $10^2$  and  $10^8$  GeV as a function of  $\ln(E/\text{GeV})$  using a constant (negative) slope.

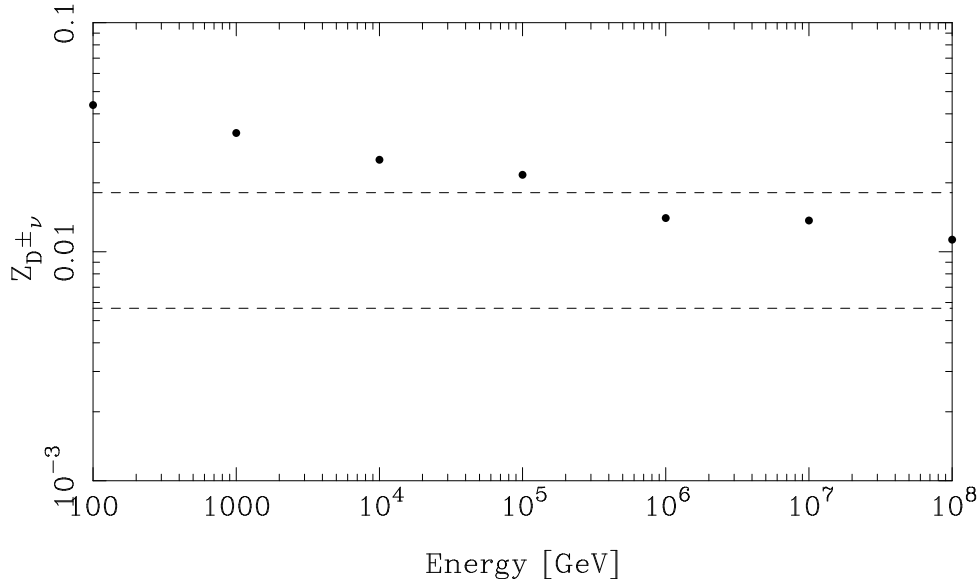


Fig. 1. The points indicate the decay moment  $Z_{D^\pm \nu}$  evaluated using three-body phase space to distribute the neutrino energy. The upper dashed line is the TIG result using  $\beta_D = 1.7$ . The lower dashed line has  $\beta_D = 3$  [2].

Our procedure for the hadronic decay moments of the  $D$ 's is to use the same energy dependence and magnitude as the semileptonic  $D$  moments as a function of energy, with a correction to account for the different branching fractions and particle multiplicities of the hadrons. For example,

$$Z_{D^\pm K^\pm} = Z_{D^\pm \nu} \cdot \frac{\langle N_{K^\pm} \rangle B(D^\pm \rightarrow K^\pm + \text{anything})}{B(D^\pm \rightarrow \nu)} \quad (3.4)$$

The  $Z_{k_{cj}}(\beta_c = 1.7)$ -moments and the branching fractions and multiplicities used are shown in Table I. In the conversion to the appropriate Z-moments, the particle data book values for the hadronic branching fractions [12] were used. In addition, we use Mark III results on the topological branching fractions [13]. The branching fractions for  $D$ 's into kaons is in the Particle Data Book. For pions, we take the branching fraction into pions equal to the fraction of all decays which are *not* semileptonic. The kaon multiplicities for  $D^0$  and  $D^+$  decays are assumed to be  $\langle N_K \rangle = 1$ . To estimate  $\langle N_{\pi^\pm} \rangle$ , we use the charged

particle topological branching fractions. Mark III data [13] indicate that the average charged particle multiplicities for  $D^0$  and  $D^+$  range between 2.4 and 2.6. We estimate that the average *hadronic* charged particle multiplicities are between 2.1-2.4. Assuming that either  $K^\pm$ ,  $K^0$  or  $\bar{K}^0$  accompanies all charmed meson decays, and that semileptonic decays have no pions, we estimate that the average number of charged pions in the decays are between 1.5-1.8, as indicated in Table I.

#### IV. RESULTS

The parameters of Table I complete what we need to evaluate the lepton fluxes. In Figures 2 and 3, we show our resulting muon and muon neutrino (particle plus anti-particle) fluxes scaled by a factor of  $E^3$ , evaluated in the vertical direction. Our conventional, prompt and secondary fluxes are shown by the solid lines. The dashed lines are the TIG parameterizations which fit their Monte Carlo results for the conventional and prompt fluxes [2].

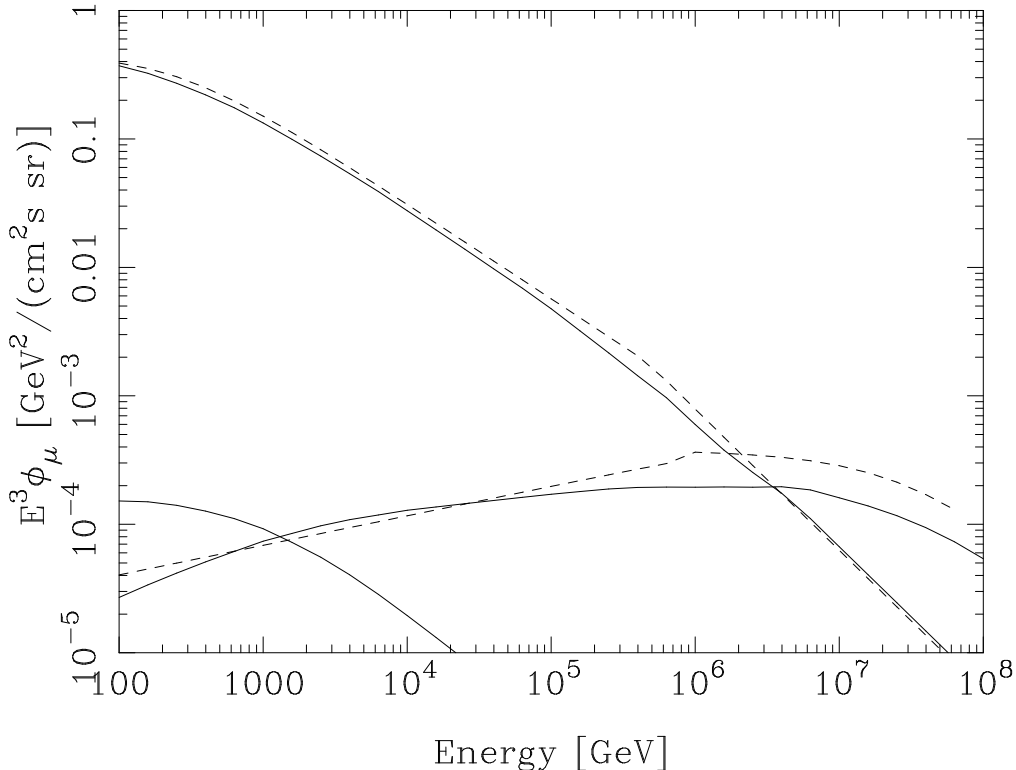


Fig. 2. The solid lines show the vertical muon plus antimuon flux, scaled by  $E^3$ , as a function on muon energy  $E$  for conventional, prompt and secondary decay sources. The dashed lines show the TIG parameterization of the conventional and prompt fluxes.

Before discussing the secondary fluxes, we comment on the discrepancies between the TIG parameterization and the prompt lepton fluxes above  $E = 10^5$  GeV. Part of the discrepancy

comes from our ignoring  $D_s$  and  $\Lambda_c$  contributions. TIG have shown that the  $\Lambda_c$ , in particular, makes significant contributions at the higher energies. In addition, while we have attempted to use the same parameters as TIG, not all of them are specified in their paper. Finally, their fit was made to Monte Carlo results, which are not exactly reproduced by this semi-analytic method using  $Z$ -moments. In any case, our focus is on secondary leptons in an energy regime where our results are in reasonable agreement with TIG's parameterizations.

We note that the secondary muon flux is larger than the prompt muon flux for  $E < 10^3$  GeV. The secondary muon neutrino flux exceeds the prompt neutrino flux only for  $E < 200$  GeV. The flux of secondary muons (and conventional muons) is larger than the corresponding neutrino flux because muons in pion decay carry the bulk of the pion's energy. For fixed energy of the lepton, the parent pion energy is lower for muons than for muon neutrinos. This is a significant feature when the parent pion flux is decreasing rapidly with energy.

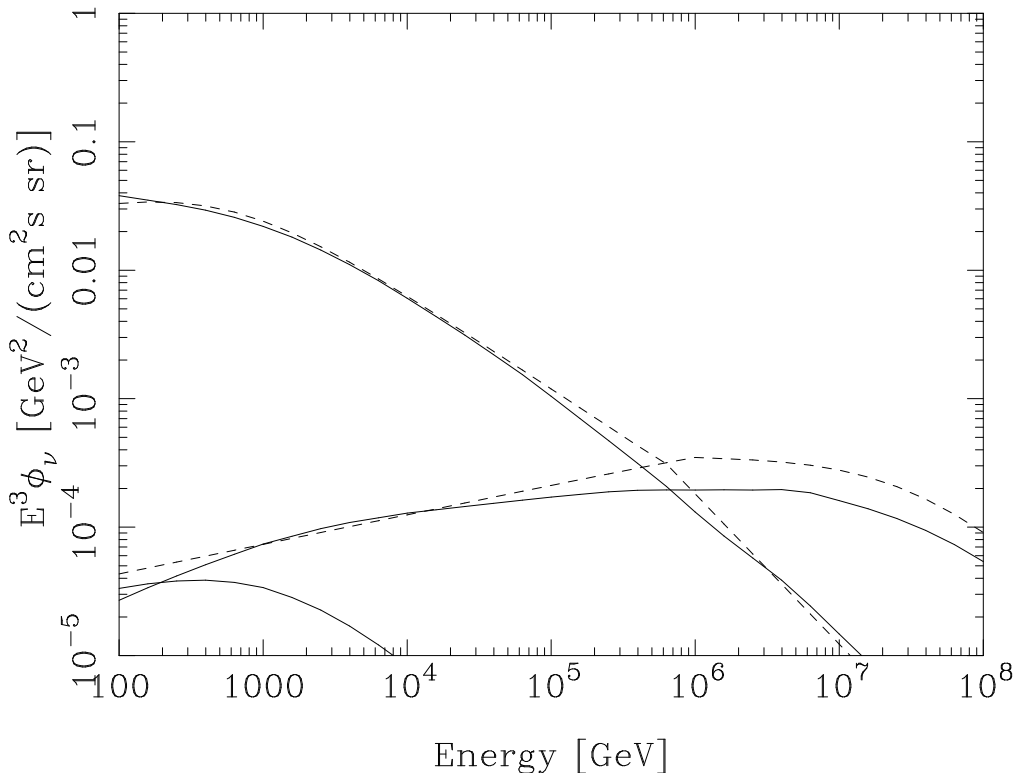


Fig. 3. The vertical muon neutrino plus antineutrino fluxes, as in Fig. 2.

The secondary  $p \rightarrow \text{charm} \rightarrow \pi, K \rightarrow \text{lepton}$  chain is suppressed by a factor of

$$R_j = \frac{\sum_{k_c} Z_{pk_c} Z_{k_c j}}{Z_{pj}} \quad (4.1)$$

relative to the conventional  $p \rightarrow \pi, K \rightarrow \text{lepton}$  chain. For TIG's calculation of charm production based on PYTHIA,  $Z_{pk_c} \sim 10^{-3} Z_{p\pi} \sim 10^{-2} Z_{pK}$ . Our secondary fluxes are suppressed by a factor of  $\sim 1/(2.4 \times 10^3)$  for muons and  $\sim 1/(1.1 \times 10^3)$  for muon neutrinos



relative to the conventional fluxes. The errors due to our approximations in the calculation of the conventional fluxes are more significant than the secondary flux as long as the charm interaction and decay moments are reliably known. We turn now to the question of whether or not the factor  $R_j$  can be increased such that the secondary flux is a significant contribution to the total flux below lepton energies of 1 TeV.

Increasing  $R_j$  may be achieved by increasing the hadronic decay moments and the interaction moments associated with the production of  $D$ 's. We will proceed by estimating an overall enhancement factor  $K$  with

$$K \equiv K_d K_\sigma K_x , \quad (4.2)$$

the product of enhancement in decay ( $d$ ), cross section ( $\sigma$ ) and in the charm energy distribution ( $x = E_c/E_p$ ), which may multiply  $R_j$ . We'll assume that these are universal to all  $R_j$ . For the limited energy range where secondary lepton fluxes are larger than prompt fluxes:  $E = 10^2 - 10^3$  GeV, we take  $K$  independent of energy. A full numerical study of the uncertainty in the charm production moments as a function of energy is in progress [14].

As described in Sec. III, we have evaluated the decay moments by rescaling the  $V - A$   $Z_{D\nu}$  moments according to multiplicities and branching fractions. By using three body phase space, the decay moments are enhanced by a factor of 2.4 at  $E = 10^2$  GeV. We take  $K_d = 2.4$ .

The cross section at next-to-leading order (NLO) in QCD is not very well specified because of the low mass of the charm quark. A variation of the charm quark mass between 1.2 and 1.8 GeV, and the renormalization scale between  $m_c/2$  and  $2m_c$  in the NLO cross section gives a range of cross sections that vary by more than two orders of magnitude [15]. By comparing the TIG cross section with fixed target cross section results, a factor  $K_\sigma = 2$  is not unreasonable.

The  $x$  distribution is an important input into the calculation of the interaction  $Z$ -moments because of the steeply falling fluxes. The quantity  $x = E_c/E_p$  defined in the fixed target frame is approximately equal to  $|x_F| \equiv 2 |p_{\parallel}^{cm}| / \sqrt{s}$ , in terms of the longitudinal momentum of the charmed quark or antiquark in the hadron center-of-momentum frame. The theoretical (perturbative QCD) distributions in  $x_F$  are typically softer than the measured distributions, which would tend to lower the predicted  $Z$ -moment. The  $x_F$  distributions for  $x_F > 0$  are parameterized by  $d\sigma/dx_F \sim (n+1)(1-x_F)^n$ . We make the scaling assumption so that the interaction  $Z$ -moments are proportional to

$$Z \sim \int_0^1 dx x^{1.7} A_n (1-x)^n \quad (4.3)$$

for the proton flux proportional to  $E^{-2.7}$  and normalization factor  $A_n = n+1$ . For low mass charmed quarks ( $m_c = 1.2$  GeV), the NLO calculations of the  $x_F$  distributions, fit to a  $(1-x_F)^n$  form, give  $n \simeq 6 - 9.5$  for  $E = 10^2 - 10^3$  GeV [15]. Fixed target data yield  $n \simeq 4.9 - 8.6$  [16], some with large error bars. To estimate  $K_x$ , we take the NA32 value for  $n$ ,  $n = 5.5$  [17] for a typical experimental value, and  $n = 7.5$  as representative of the perturbative value, so

$$K_x = \frac{\int_0^1 dx x^{1.7} 6.5 (1-x)^{5.5}}{\int_0^1 dx x^{1.7} 8.5 (1-x)^{7.5}} = 1.5 . \quad (4.4)$$

Taken together, the overall enhancement factor based on modifications to the TIG charm production parameters is on the order of  $K \sim 7$ .

Intrinsic charm, in principle, may boost the charm production rate. Intrinsic charm models have a charm (and anti-charm) component in the proton at a low scale  $Q_0$ , before QCD evolution has generated  $c\bar{c}$  pairs by gluon splitting [18]. Estimates of the  $Z$ -moments for several models of intrinsic charm were made by TIG [2], and maximum  $Z$ -moments of a few times  $10^{-3}$  were found. These are at just the level of the perturbative charm  $Z$ -moments, so again, may account for at most a factor of two.

Finally, we turn to a model which does not rely exclusively on the perturbative parameters presented by TIG and energy independent modifications. We use a charm cross section at high energies suggested by Zas, Halzen and Vázquez [19] where

$$\sigma_{c\bar{c}} = 0.1\sigma_{tot} , \quad (4.5)$$

where  $\sigma_{tot}$  appears in Eq. (3.2). The form of the cross section in Eq. (4.7) seriously overestimates the cross section in the measured regime,  $E = 10^2 - 10^3$  GeV. We take the hadronic production cross section to be

$$\sigma_{c\bar{c}} = \frac{\sigma_{c\bar{c}}^{LE} \cdot 0.1\sigma_{tot}}{\sigma_{c\bar{c}}^{LE} + 0.1\sigma_{tot}} \quad (4.6)$$

where  $\sigma_{c\bar{c}}^{LE}$  is the next-to-leading order perturbative cross section with  $m_c = 1.3$  GeV, evaluated at the renormalization and factorization scales set to  $\mu = m_c$ , for  $E \leq 10^3$  GeV, using the CTEQ3 parton distribution functions [20]. This is a slight overestimate of the data below  $E = 10^3$  GeV. Above  $10^3$  GeV, we take a power law

$$\sigma_{c\bar{c}}^{LE} = 1.3 \cdot 10^5 (E/\text{GeV})^{0.865} \text{ pb} , \quad (4.7)$$

which is the power law extrapolation of the perturbative cross section at  $E = 10^3$  GeV.

By  $E \sim 10^6$  GeV,  $\sigma_{c\bar{c}} \sim 0.1\sigma_{tot}$ . This assumption yields significantly higher prompt fluxes at high energies. Indeed, Gonzalez-Garcia, Halzen, Vázquez and Zas [21] have shown that such large charm cross sections above energies of  $10^5$  GeV are problematic when one looks at Akeno horizontal air shower data [22]. For our purposes here, we are interested in the cross section only as it affects the interaction  $Z$ -moments below 1-10 TeV. For the  $x$  distribution, we assume a scaling form,  $d\sigma/dx \sim 5(1-x)^4$ , which is consistent with measured values [23]. Using these inputs, our results for the prompt and secondary muon fluxes from charm decay are shown with the dashed lines in Fig. 4. For comparison, the solid lines indicate the TIG results and our secondary flux calculation based on TIG parameters, as in Fig. 2. The difference between the fluxes at  $E = 10^2$  GeV are due to differences in total cross sections and  $x$ -distributions relative to PYTHIA generated distributions.

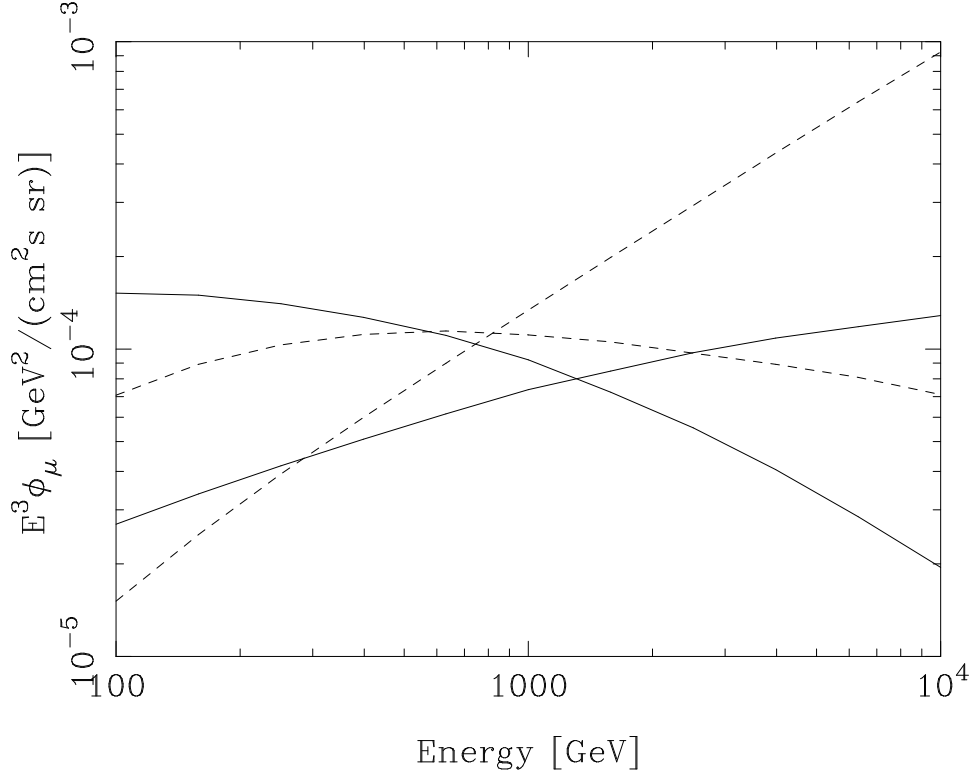


Fig. 4. The vertical muon prompt and secondary muon fluxes, scaled by  $E^3$ , using the conventional TIG parameters (solid line) and using Eq. (4.8) and  $d\sigma/dx \sim 5(1-x)^4$  (dashed line).

It is clear from Fig. 4 that at energies above a few TeV, the high energy behavior of the cross section and  $x$ -distribution have important implications for the prompt neutrino flux. Recall that at these energies, the prompt muon flux equals the prompt muon neutrino flux, and also equals the prompt electron neutrino flux. The prompt fluxes are isotropic. For the enhanced prompt flux of Fig. 4, the crossover from the vertical conventional-dominated to prompt-dominated muon neutrino fluxes occurs around  $E \sim 3 \cdot 10^4$  GeV. This is in contrast to TIG's result of a crossover close to  $E \sim 10^6$  GeV. However, there is no significant effect for  $E < 10^3$  GeV using the enhanced cross sections, given our overall uncertainty of a factor of  $K \sim 10$ . Indeed, below  $E = 10^4$  GeV, a factor of 10 uncertainty in the lepton fluxes from charm decay is a reasonable estimate.

Finally, we remark that while we have focussed on secondary leptons in the energy interval 100-1000 GeV, it is interesting to note that the dashed line in Fig. 4, if valid at  $E = 10^4$  GeV, has important implications for the electron neutrino flux. At  $E = 10^4$  GeV, the prompt muon neutrino flux is still an order of magnitude below the vertical conventional flux, however, the prompt electron neutrino flux is larger than the vertical conventional flux. This can be seen by considering the ratio  $R \equiv \phi_{\nu_\mu}/\phi_{\nu_e}$  as a function of zenith angle  $\theta$  and energy. Using the Bartol group's calculation of the conventional atmospheric lepton fluxes [24], neglecting any charm contribution, the ratios are:

$$R_{no\ c}(E_\nu = 10^4 \text{ GeV}, \cos \theta = 1) = 32 \quad (4.8)$$

$$R_{no\ c}(E_\nu = 10^4 \text{ GeV}, \cos\theta = 0) = 29 .$$

However, when one adds in the prompt flux shown by the dashed line in Fig. 4, the same ratios yield

$$\begin{aligned} R_{with\ c}(E_\nu = 10^4 \text{ GeV}, \cos\theta = 1) &= 7 \\ R_{with\ c}(E_\nu = 10^4 \text{ GeV}, \cos\theta = 0) &= 18 . \end{aligned} \tag{4.9}$$

Measuring  $R$  is a difficult task, especially at 10 TeV, because of the difficulty of measuring the electron neutrino flux. Air shower arrays are, in principle, sensitive to electron neutrino induced events, however, acceptances are low compared with higher energies [25]. In underground experiments, one does not have the advantage of the long muon range that increases the effective volume of the detector when the process is  $\nu_e N$  charged-current interactions.

## V. CONCLUSIONS

We have focused here on corrections to the atmospheric lepton fluxes from charm decays in the energy range  $E = 10^2 - 10^3$  GeV, where secondary neutrinos from the  $D \rightarrow K, \pi \rightarrow \nu_\mu, \mu$  decay chain contribute. The secondary flux corrections are significant for the muon flux compared to the prompt muon flux below  $\sim 10^3$  GeV, and for the muon neutrino fluxes below  $\sim 200$  GeV. Since the branching fraction for  $K^\pm$  and  $\pi^\pm$  decays to electron neutrinos is small, secondary corrections to the atmospheric electron neutrino fluxes is negligible.

The prompt and secondary lepton fluxes are tied to the charm cross section and energy distribution of the emerging charmed particles. We have demonstrated here that the experimental constraints on the charm production cross section and energy distribution limit the extent to which leptons from the decays of charm can contribute to the overall atmospheric lepton fluxes. Taking the parameters of TIG in Ref. [2] as a starting point, we have shown that the uncertainties in the calculation of the lepton fluxes from charm decay may result in an enhancement by as much as a factor of 10 in the energy range of  $10^2 - 10^3$  GeV. An additional two orders of magnitude are required to make the secondary lepton fluxes comparable to the conventional ones at  $E = 100$  GeV. At higher energies, where one is less constrained by experiments, the high energy behavior of the charm cross section and energy distribution significantly influences the prompt flux, a topic of further investigation [14].

## ACKNOWLEDGMENTS

Work supported in part by National Science Foundation Grant No. PHY-9507688, a University of Iowa CIFRE Award and D.O.E. Contract No. DE-FG02-95ER40906. M.H.R. acknowledges the hospitality of the CERN Theory Division where this work was completed. We thank P. Nason and M. Mangano for useful discussions.

## REFERENCES

- [1] L. V. Volkova, *Yad. Fiz.* **31**, 1510 (1980) [English translation: *Sov. J. Nucl. Phys.* **31**, 784 (1980)]; K. Mitsui, Y. Minorikawa and H. Komori, *Nuo. Cim.* **9c**, 995 (1986); A. V. Butkevich, L. G. Dedenko and I. M. Zheleznykh, *Yad. Fiz.* **50**, 142 (1989) [English translation: *Sov. J. Nucl. Phys.* **50**, 90 (1990)]; V. Agrawal, T. K. Gaisser, P. Lipari and T. Stanev, *Phys. Rev.* **D53**, 1314 (1996); L. V. Volkova and G. T. Zatsepin, *Yad. Fiz.* **37**, 353 (1983); H. Inazawa and K. Kobayakawa, *Prog. Theor. Phys.* **69**, 1195 (1983); P. Pal and D. P. Bhattarcharyya, *Nuo. Cim.* **C15**, 401 (1992).
- [2] M. Thunman, P. Gondolo and G. Ingelman, *Astropart. Phys.* **5**, 309 (1996).
- [3] K. Daum et al., Fréjus Coll., *Z. Phys.* **C66**, 417 (1995).
- [4] D. J. Bird et al., *Phys. Rev. Lett.* **71**, 3401 (1993), *Astrophys. J.* **424**, 491 (1994); S. Yoshida et al., *Astropart. Phys.* **3**, 105 (1995); N. Hayashida et al., *Phys. Rev. Lett.* **73**, 3494 (1994).
- [5] R. Gandhi, C. Quigg, M. H. Reno and I. Sarcevic, *Astropart. Phys.* **5**, 81 (1996).
- [6] See, e.g., A. M. Hillas, *Ann. Rev. Astron. Astrophys.* **22**, 425 (1984).
- [7] T. Sjöstrand, *Comput. Phys. Commun.* **82**, 74 (1994).
- [8] P. Lipari, *Astropart. Phys.* **1**, 195 (1993).
- [9] T. K. Gaisser, *Cosmic Rays and Particle Physics*, (Cambridge University Press, New York, 1990).
- [10] T. H. Burnett et al., (JACEE Collaboration), *Ap. J.* **349**, L25 (1990).
- [11] A. Donnachie and P. V. Landshoff, *Phys. Lett. B* **296**, 227 (1992).
- [12] R. M. Barnett et al., *Phys. Rev.* **D54**, 1 (1996).
- [13] D. Coffman et al. (Mark III Collaboration), *Phys. Lett. B* **263**, 135 (1991).
- [14] L. Pasquali, M. H. Reno and I. Sarcevic, in progress.
- [15] S. Frixione, M. L. Mangano, P. Nason and G. Ridolfi, *Nucl. Phys.* **B431**, 453 (1994). See also the review by S. Frixione et al., e-print archive hep-ph/9702287, to be published in *Heavy Flavours II*, edited by A. J. Buras and M. Lindner, World Scientific.
- [16] J. Appel, *Ann. Rev. Nucl. Part. Sci.* **42**, 367 (1992).
- [17] S. Barlag et al., ACCMOR Coll., *Z. Phys.* **C39**, 451 (1988).
- [18] S. J. Brodsky, P. Hoyer, C. Peterson and N. Sakai, *Phys. Lett.* **B93**, 451 (1980); S. J. Brodsky and C. Peterson, *Phys. Rev.* **D23**, 2745 (1981).
- [19] E. Zas, F. Halzen and R. A. Vázquez, *Astropart. Phys.* **1**, 297 (1993).
- [20] H. L. Lai et al. (CTEQ Collaboration), *Phys. Rev.* **D51**, 4763 (1995).
- [21] M. C. Gonzalez-Garcia, F. Halzen, R. A. Vázquez and E. Zas, *Phys. Rev.* **D49**, 2310 (1994).
- [22] M. Nagano et al., *J. Phys. G* **12**, 69 (1986).
- [23] See Ref. [15] for a summary of the experimental results.
- [24] V. Agrawal et al., *Phys. Rev.* **D53**, 1314 (1996).
- [25] For acceptances estimated for the Pierre Auger detector, see, for example, G. Parente and E. Zas, e-print archive astro-ph/9606091.

TABLES

TABLE I. Charmed particle decay moments.

Decaying Particle ( $k_c$ )	$i$	$B$	$\langle N_i \rangle$	$Z_{k_c i}(\beta_c = 1.7)$
$D^+$	$K^\pm$	0.30	1	0.032
	$K_L$	0.30	1	0.032
	$\pi^\pm$	0.66	1.5	0.10
	$\nu_\mu, \bar{\nu}_\mu$	0.17	1	0.018
$D^0$	$K^\pm$	0.56	1	0.069
	$K_L$	0.21	1	0.026
	$\pi^\pm$	0.85	1.8	0.19
	$\nu_\mu, \bar{\nu}_\mu$	0.068	1	0.0084